Crystalline ice growth on Pt(111) and Pd(111): Nonwetting growth on a hydrophobic water monolayer

Greg A. Kimmel, Nikolay G. Petrik, Zdenek Dohnálek, and Bruce D. Kay

Citation: The Journal of Chemical Physics **126**, 114702 (2007); doi: 10.1063/1.2672869
View online: http://dx.doi.org/10.1063/1.2672869
View Table of Contents: http://scitation.aip.org/content/aip/journal/jcp/126/11?ver=pdfcov
Published by the AIP Publishing

Crystalline ice growth on Pt(111) and Pd(111): Nonwetting growth on a hydrophobic water monolayer

Greg A. Kimmel,[a),b)] Nikolay G. Petrik, Zdenek Dohnálek, and Bruce D. Kay[a),c)]
Chemical and Materials Sciences Division, Pacific Northwest National Laboratory, P.O. Box 999, Richland, Washington 99352

(Received 25 September 2006; accepted 19 January 2007; published online 16 March 2007)

The growth of crystalline ice films on Pt(111) and Pd(111) is investigated using temperature programed desorption of the water films and of rare gases adsorbed on the water films. The water monolayer wets both Pt(111) and Pd(111) at all temperatures investigated [e.g., 20–155 K for Pt(111)]. However, crystalline ice films grown at higher temperatures (e.g., $T>135$ K) do not wet the monolayer. Similar results are obtained for crystalline ice films of D_2O and H_2O. Amorphous water films, which initially wet the surface, crystallize and dewet, exposing the water monolayer when they are annealed at higher temperatures. Thinner films crystallize and dewet at lower temperatures than thicker films. For samples sputtered with energetic Xe atoms to prepare ice crystallites surrounded by bare Pt(111), subsequent annealing of the films causes water molecules to diffuse off the ice crystallites to reform the water monolayer. A simple model suggests that, for crystalline films grown at high temperatures, the ice crystallites are initially widely separated with typical distances between crystallites of ~14 nm or more. The experimental results are consistent with recent theory and experiments suggesting that the molecules in the water monolayer form a surface with no dangling OH bonds or lone pair electrons, giving rise to a hydrophobic water monolayer on both Pt(111) and Pd(111). © *2007 American Institute of Physics*.
[DOI: 10.1063/1.2672869]

I. INTRODUCTION

The structure of water at interfaces influences the physical, chemical, and biological processes relevant to a large number of natural and man-made systems. As a result, the structure of water at—and its interactions with—surfaces have been extensively studied. For example, the structures of submonolayer and monolayer (ML) water films on surfaces such as metals, oxides, and semiconductors have been investigated with a variety of surface science techniques.[1–3] The gross structure (e.g., the contact angle) of macroscopic amounts of water and ice on various hydrophobic and hydrophilic substrates has also been investigated for years.[4]

In contrast, much less is known about the morphology of nanometer scale water films (i.e., coverages greater than 1 ML). Scanning tunneling microscopy (STM) and atomic force microscopy have been used to investigate nanoscale water films on a few systems such as Cu(111), Au(111), and mica.[5–7] The morphology of nanoscale amorphous solid water (ASW) films has also been investigated with optical interferometry[8,9] and physisorption/desorption techniques.[9–11] Verdaguer *et al.* have recently reviewed the existing literature on the structure of thin water films.[3]

Here we investigate the growth of crystalline ice (CI) films on Pt(111) and Pd(111) using temperature programed desorption (TPD) of both water and Kr adsorbed on the water films. The water monolayer wets Pt(111) (Refs. 12–14) and Pd(111).[15] However, for coverages greater than 1 ML, the additional water molecules form ice crystallites that do not wet the water monolayer, portions of which remain exposed even for total coverages as large as ~45 ML. Similar results are obtained for both H_2O and D_2O films, indicating that there is no significant isotope effect for water films on Pt(111) and Pd(111). Thin ASW films which wet the surface[16] typically dewet when the films crystallize upon annealing. A simple model suggests that initially the ice crystallites are widely separated with typical lateral spacings of 14 nm or more. The structure of the water monolayer on Pt(111) and Pd(111), which has no dangling OH bonds or lone pair electrons, is key to understanding the nonwetting growth of CI films.[17,18] The fully coordinated water monolayer results in a *hydrophobic* surface on which water diffusion is facile. At high temperatures, where large scale rearrangement of the films is *kinetically* accessible, the low surface energy of the hydrophobic water monolayer relative to the crystalline ice surface *thermodynamically* favors the formation of nonwetting, three dimensional (3D) ice crystallites. The hydrophobic character of the water monolayer is further supported by the observation that kinetically wetted amorphous films dewet upon heating, exposing the water monolayer.

II. EXPERIMENT

The majority of the experiments reported here were performed in an ultrahigh vacuum chamber with a base pressure of $\sim 1\times 10^{-10}$ Torr that was equipped with a molecular beam, a quadrupole mass spectrometer, a closed-cycle he-

[a)]Authors to whom correspondence should be addressed.
[b)]Electronic mail: gregory.kimmel@pnl.gov
[c)]Electronic mail: bruce.kay@pnl.gov

lium cryostat, and an Auger electron spectrometer. The Pt(111) sample was resistively heated, and the temperature was measured with a K-type thermocouple. The sample was cleaned by sputtering with 2 keV Ne^+ followed by annealing to ~1000 K. After flashing to high temperatures (~1000–1100 K), the sample cooled to ~40 K in less than 200 s.

The water films were grown at normal incidence using a molecular beam that was smaller than and centered on the Pt(111) with a flux corresponding to ~0.2 ML/s. The central portion of the water films, where the coverage was constant (the umbra), accounted for ~87% of the total area of the water films on the substrate, with the penumbra (where the coverage decreases to zero) accounting for the rest. The nonconstant coverage in the penumbra does not qualitatively alter any of the results presented below and produces only minor quantitative changes. For example, experiments using a rare gas probe beam, with a diameter that was smaller than the umbra of the water film, gave similar results to those where the water and rare gas beams were the same size.

Water TPD spectra indicative of a clean surface with few defects were routinely observed.[13] The first monolayer of water wets Pt(111) (Refs. 12–14 and 19) and desorbs at a higher temperature than multilayers of water.[13] Therefore, the coverage corresponding to 1 ML of water can be determined by the onset of multilayer desorption. We estimate the uncertainty in our ML coverage calibration to be ±0.05 ML. With the monolayer coverage calibration, other coverages are determined by comparing the integrals of their TPD spectra to that of the monolayer. Using this approach, the total coverage was accurately determined (to within ±3%) for small coverages (e.g., $\theta < 5$ ML). After water deposition, the sample was cooled to low temperature (typically 20–30 K) and dosed with Kr using the same molecular beam source. Kr TPD spectra were obtained using a heating rate of 0.5 K/s. The results shown below are primarily for D_2O on Pt(111). However, similar results have been obtained for H_2O on Pt(111) and also for water growth on a thin (~4 ML) epitaxial Pd(111) film grown on top of Pt(111).[20,21] Furthermore, the main results have been verified on two separate experimental instruments, each using a different Pt(111) crystal.

III. RESULTS AND DISCUSSION

A. Nonwetting growth of crystalline ice films

We have previously shown that the desorption of rare gas atoms can be used to investigate the morphology of thin water films grown on Pt(111) and Pd(111).[16,22] The basic idea is that the temperature at which a rare gas atom desorbs can be used to assess the height of the atom above a metal surface.[23–25] The temperature at which the atom desorbs is related to the chemical potential of the adsorbate layer, which, in turn, is set by the highest layer in the film (i.e., the layer furthest from the substrate) which is occupied by the adsorbates. This approach can be used to assess the height of a rare gas atom—Kr for the results presented here—adsorbed on a thin film of water grown on a metal substrate. The interaction of Kr adsorbed on a multilayer crystalline ice surface is weaker than for Kr adsorbed on Pt(111) or Pd(111), or on one layer of water on those substrates. Therefore the peak in Kr TPD spectra associated with crystalline ice occurs at lower temperatures than the Kr TPD peak for either the water monolayer or the bare metal substrate.

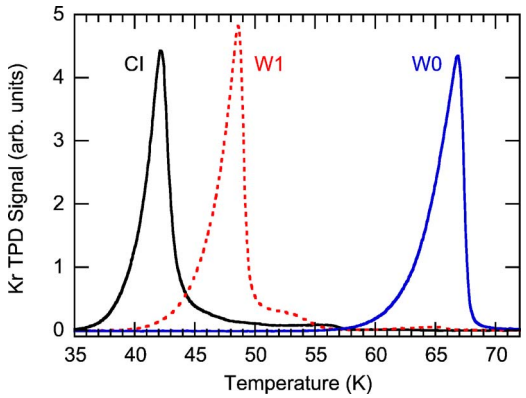

FIG. 1. (Color online) Kr TPD spectra from Pt(111) (W0), 1 ML of water on Pt(111) (W1), and ~50 ML crystalline ice on Pt(111) (CI). For each TPD spectrum,~1 ML of Kr was adsorbed on the surface and the temperature ramp rate was 1 K/s. The well-resolved TPD peaks allow the morphology of thin crystalline ice films to be investigated.

Figure 1 shows the TPD spectra of ~1 ML Kr desorbing from bare Pt(111) (labeled W0 in the figure), a monolayer of D_2O on Pt(111) (W1), and multilayer crystalline D_2O (CI). In each case, the Kr primarily desorbs in a single peak. Since the polarizability of a water film is smaller than the Pt(111) substrate and the water films separate the Kr from the Pt(111), the Kr desorption temperatures from both one layer of water and multilayer CI films are lower than that from Pt(111). The differences in the Kr spectra evident in Fig. 1 form the basis for analyzing the growth of crystalline ice films on Pt(111). Analogous results apply for the Kr TPD spectra of water on Pd(111).

Since the first layer of water wets Pt(111) (Refs. 12, 13, 19, 26, and 27) and Pd(111),[15,28,29] the amount of Kr desorption from bare Pt(111) decreases linearly and the amount desorbing from one layer of water increases linearly as the water coverage increases from 0 to 1 ML for a wide range of water adsorption temperatures (~30–155 K).[16,22] However, for higher coverages, the morphology of the film depends on the growth temperature: ASW films grown at normal incidence uniformly cover (i.e., "wet") the water monolayer,[16,30] while crystalline ice films do not.[22] The nonwetting growth of CI films on the water monolayer is demonstrated in Fig. 2, which shows a series of Kr TPD spectra from D_2O and H_2O CI films on Pt(111) and Pd(111) for various water coverages. For water coverages greater than 1 ML, the W1 TPD peak decreases and the CI peak increases as the water coverage increases. On both substrates, the Kr TPD spectra have a well-defined isosbestic point [at 44.0 K on Pt(111) and 45.0 K on Pd(111)], indicating that the spectra are composed of two overlapping features which convert from one to the other as the water coverage increases. The key observation is that on both Pt(111) and Pd(111), large coverages of CI are required before Kr desorption from the water monolayer is no longer observed.

The Kr TPD peaks due to desorption from the ice crys-

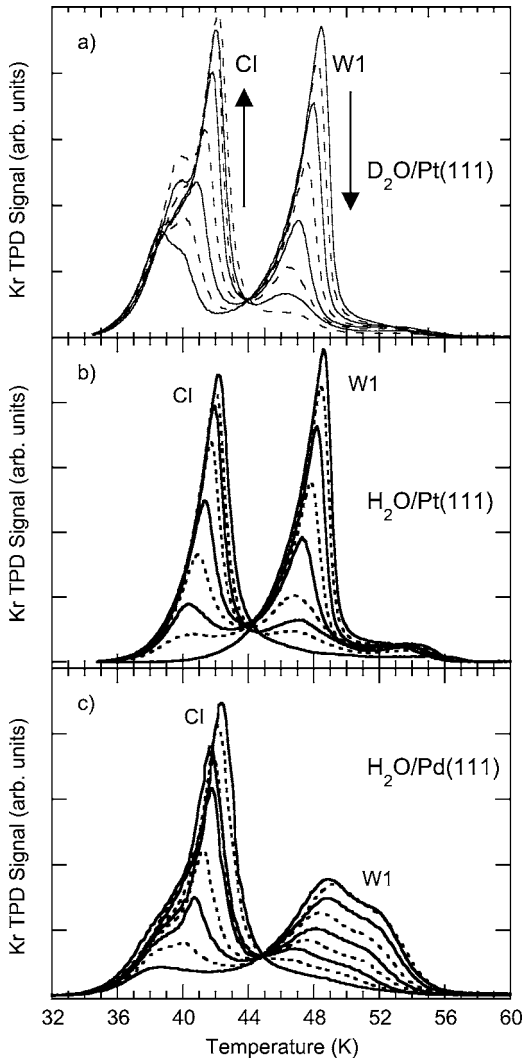

FIG. 2. Kr TPD spectra for various crystalline ice films on Pt(111) and Pd(111). In each case ~1 ML of Kr is adsorbed on the surface and the temperature ramp rate was 1 K/s. (a) crystalline D_2O on Pt(111) deposited at 152 K for coverages from 1 to 50 ML, (b) crystalline H_2O on Pt(111) deposited at 145 K for coverages from 1 to 45 ML, and (c) crystalline H_2O on Pd(111) deposited at 150 K for coverages from 1 to 96 ML. On both Pt(111) and Pd(111), large total coverages are required before the W1 TPD peak, corresponding to Kr desorbing from one layer of water, disappears.

tallites are essentially the same on both Pt(111) and Pd(111) as expected (T_{peak}=42.2 K for surfaces fully covered with crystalline ice). For both the D_2O/Pt(111) and H_2O/Pd(111) data [Figs. 2(a) and 2(c)], the total Kr coverage is slightly greater than 1 ML, resulting in the shoulder observed on the low-temperature side of the CI peak. For the H_2O/Pt(111) data [Fig. 2(b)], the Kr dose was slightly less and this low-temperature shoulder is absent.

The high-temperature portion of the Kr TPD spectra from water on Pd(111) [Fig. 2(c)] appears to be more complicated than from water on Pt(111) [Figs. 2(a) and 2(b)]: On Pd(111), the Kr TPD spectra from the water monolayer have a prominent shoulder on the high-temperature side of the main peak. The Kr TPD spectra from the water monolayer on Pt(111) also have a shoulder on the high-temperature side of the main peak, but the intensity of the feature is much larger on Pd(111). In addition, on both surfaces, there is a small peak (not shown) at even higher temperatures (in the range of desorption from the bare substrate, ~62 K), which is also larger on Pd(111), but still only a small fraction of the total Kr desorption. The origin of these features is not clear. However, the results suggest that for the water monolayer on Pd(111), there are two Kr adsorption sites with two different binding energies. One possibility is that, even though the lattice constants for Pd and Pt differ by only 0.8%, the structure of the water monolayers is different on Pt(111) and Pd(111). While the structure of the complete water monolayer on Pd(111) is not known in detail, the structure of submonolayer water islands is apparently quite different on the two surfaces: On Pd(111), complicated islands that are based on a commensurate $(\sqrt{3}\times\sqrt{3})R30°$ structure form.[15] However, on Pt(111), islands form with a $(\sqrt{37}\times\sqrt{37})R25°$ structure that is compressed relative to the $(\sqrt{3}\times\sqrt{3})R30°$ overalyer.[12,27] Despite the differences in the Kr TPD line shapes of Pt(111) and Pd(111), the high-temperature monolayer desorption is well separated from the CI desorption peak on both surfaces and can be used to quantify the fraction of the surface covered by only one layer of water, F_1.

From the results such as those shown in Fig. 2, F_1 can be calculated as a function of the water coverage by first integrating the Kr TPD spectra for temperatures greater than the isosbestic point (i.e., by integrating over the W1 peak in the TPD spectra). However, since the CI and monolayer components of the Kr TPD spectra overlap, it is necessary to subtract the contribution of the CI component from the integral. Since we do not know *a priori* how the CI and monolayer components of the Kr TPD, spectra evolve as the total coverage increases, we approximate the CI contribution to the integral. We have done this by assuming that the CI background is proportional to the integral over the low-temperature portion of the TPD, where the CI signal is dominant (for coverages greater than 1 ML). Other approaches for approximating the CI contribution to the integral over the W1 peak give qualitatively similar results.

For coverages greater than 1 ML, F_1 vs θ is nearly identical for both H_2O and D_2O adsorbed on Pt(111), and these are qualitatively similar to the results for H_2O on Pd(111) (Fig. 3). On both surfaces, F_1 decreases relatively quickly for water coverages less than ~12–15 ML and then more slowly at higher coverages. On Pt(111) F_1 tends to zero at ~50 ML, while for Pd(111) this occurs at ~80 ML. The inset to Fig. 3 shows in more detail F_1 vs θ for 1 ML$\leqslant\theta<$20 ML. Also shown for comparison is F_1 for amorphous D_2O films on Pt(111), where the second layer wets the water monolayer and F_1 decreases linearly for 1 ML$<\theta<$2 ML.[16] Although it is omitted here for clarity, F_1 linearly increases for $0<\theta<1$ ML for both Pt(111) and Pd(111).[16,22]

At θ=2 ML, where the water monolayer is essentially completely covered for ASW films, only ~6% of the water monolayer is covered by ice crystallites for H_2O on Pd(111) and ~15% is covered for H_2O and D_2O on Pt(111). Clearly CI does not wet the water monolayer on either substrate. At any coverage, the average height of the ice crystallites, z_{ave}, on top of the water monolayer is given by $z_{ave}=(\theta-1)/F_1$. Therefore, at θ=2 ML, z_{ave} is ~17 layers on Pd(111) and ~7 layers on Pt(111).

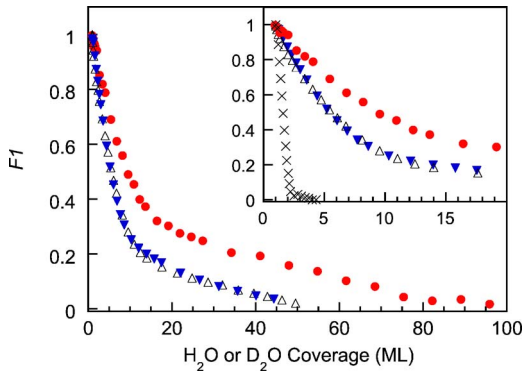

FIG. 3. (Color online) The fraction of the surface covered by one and only one layer of water, F_1, vs total water coverage for crystalline H_2O deposited at 150 K on Pd(111) (circles), crystalline D_2O deposited at 152 K on Pt(111) (open triangles), and crystalline H_2O deposited at 145 K on Pt(111) (filled triangles). Only coverages $\geqslant$1 ML are shown. Inset: F_1 vs the total water coverage for smaller coverages. In addition to the nonwetting crystalline ice films, F_1 for wetting ASW films on Pt(111) (crosses) is also shown for comparison.

In contrast to the nonwetting growth of CI films, multilayer ASW films (i.e., films grown below ~120 K) wet both Pt(111) and Pd(111).[16] At intermediate temperatures, films that wet the Pt(111) can also be grown, although the degree of long range order in these films is unclear. Figure 4 shows the TPD of ~1 ML of Kr desorbing from D_2O films grown on Pt(111) at temperatures ranging from 134 to 150 K. For these films the total D_2O coverage is ~4 ML. At 134 K, the water film completely covers the water monolayer as evidenced by the complete absence of the high-temperature TPD peak. At 136 K, a multilayer water film covers most of the surface, and only a small portion of the water monolayer is uncovered. As the growth temperature is increased beyond 136 K, more and more water monolayer becomes exposed. We have also measured F_1 vs θ at lower growth temperatures than for the results in Fig. 3 and found that F_1 decays more rapidly as the coverage increases (data not shown), in agreement with the results in Fig. 4.

While we do not know the equilibrium configuration for

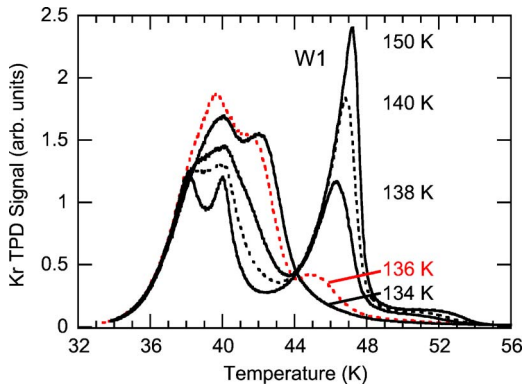

FIG. 4. (Color online) Kr TPD spectra for ~4 ML D_2O deposited on Pt(111) at the temperatures indicated in the figure. For growth temperatures at or below 134 K, the W1 Kr TPD peak is absent indicating that no portion of the surface is covered by only one layer of water. As the growth temperature is increased, the W1 TPD peak increases as the ice crystallites progressively cover less of the water monolayer. (For the film grown at 150 K, the total coverage is less than 4 ML due to water desorption during film growth.)

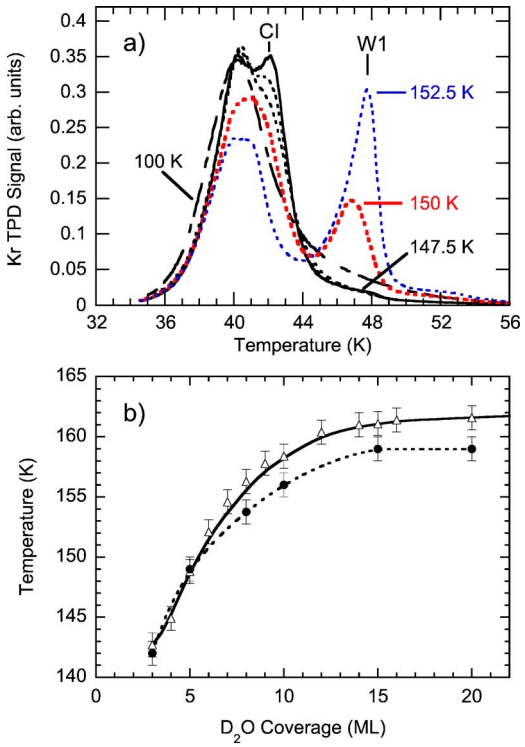

FIG. 5. (a) (Color online) Kr TPD spectra for a 5 ML film grown at 100 K on Pt(111) that was subsequently annealed to various temperatures as indicated in the figure. For annealing temperature $\leqslant$147 K, the multilayer water films still cover the surface. For annealing to 147 K, the film has begun to crystallize. For higher temperatures, the films begin to dewet the surface as evidenced by the appearance of the W1 Kr TPD peak. (b) Dewetting temperature (circles) and crystallization temperature (triangles) vs total water coverage for initially amorphous D_2O films grown at 100 K on Pt(111).

an ice film on Pt(111) or Pd(111) at any given temperature, the results in Fig. 4 show that the fraction of the surface covered by ice crystallites depends strongly on the growth conditions. The low-temperature region of the Kr TPD spectra exhibits a complicated line shape over this range of growth temperatures for several reasons. First, the films grown in this temperature range are a mixture of crystalline and amorphous phases. Second, the fraction of the surface covered by the ice crystallites changes dramatically over this temperature range. As shown elsewhere,[31,32] the TPD line shapes for physisorbed species are different for CI and ASW films. Taken together, these effects result in the complicated Kr TPD line shapes observed below the isosbestic point (T =44 K) in Fig. 4.

B. Dewetting of ASW films upon crystallization

For wetting films grown at lower temperatures, the films eventually dewet when heated to higher temperatures, exposing the water monolayer but not bare Pt(111) or Pd(111). Figure 5(a) shows a series of Kr TPD spectra from 5 ML D_2O films dosed at 100 K that have been annealed to various temperatures. The as-grown film is amorphous and, since there is no TPD peak associated with Kr desorption from the water monolayer, it completely covers the water monolayer (dot-dashed line). For films that have been annealed, a peak in the Kr TPD spectra at ~42 K due to Kr desorbing from CI begins to develop prior to the appearance of the W1 peak

(e.g., T_{anneal}=147.5 K, solid line). This indicates that, for this coverage, the films begin to crystallize prior to dewetting. However, annealing the film to just a little higher temperature leads to dewetting (T_{anneal}=150 K, dotted line). Note that initially wetting films dewet at annealing temperatures that are higher than the temperatures required to grow nonwetting CI films [compare Figs. 4 and 5(a)]. This result is plausible, since it should be easier for newly adsorbed molecules to adopt the energetically preferred configuration compared to molecules already incorporated into an ASW film at lower temperatures.

The temperature at which ASW films dewet the water monolayer, T_d, increases with coverage from ~3 to 20 ML [Fig. 5(b), circles]. For these experiments, ASW films were deposited at 100 K, the temperature was then ramped at 1 K/s to a given temperature, at which point the heater was shut off, and the sample free cooled (at ~2 K/s) to the base temperature (~28 K) after which a Kr TPD spectrum was obtained. This procedure was repeated for freshly deposited films at a variety of annealing temperatures to determine the temperature at which the films began to dewet the water monolayer based on the appearance of the W1 peak in the Kr TPD spectra [e.g., Fig. 5(a)].

The approximate temperature at which water films crystallize, T_c, can also be tracked based on the water TPD spectra.[26,33,34] Since the desorption rates from ASW and CI differ by a factor of ~2 for the temperatures relevant for desorption experiments,[26,34] the decrease in desorption rate when the film crystallizes is easy to discern. Figure 5(b) (triangles) shows T_c as a function of film thickness. In this case, T_c is taken as the temperature at which the desorption rate is midway between the ASW and CI desorption rates (presumably corresponding to the film surface being approximately 50% crystallized). The coverage dependences of T_c and T_d are quite similar, suggesting a strong correlation between these processes. Inspection of the Kr TPD for thicker films (e.g., ~15 ML) indicates that the films dewet as they begin to crystallize. Therefore T_d is typically somewhat less than T_c in Fig. 5(b), since T_c corresponds to a temperature at which ~50% of the film surface is crystalline. In fact, none of the evidence suggests that thin water films begin to dewet prior to the onset of crystallization.

The results in Fig. 5 show that dewetting of the films is typically correlated with crystallization. However, for ASW films on Pt(111) that are annealed at relatively low temperatures (e.g., 130 K), it is possible to crystallize the film without substantial dewetting.[31,32] These crystallized films, which cover the substrate, are metastable, since they dewet upon heating to higher temperatures (data not shown). Thus crystallization is apparently a necessary but not a sufficient condition for dewetting. Previous results have suggested that it is energetically favorable for ASW films to wet both Pt(111) and Pd(111),[16] and the observation that crystallization apparently precedes dewetting also supports this conclusion.

We have also investigated the crystallization and dewetting of ASW films that are annealed isothermally. For isothermal annealing at lower temperatures (T<140 K), the films typically crack during crystallization but do not substantially dewet the surface.[32,35] However, at higher isothermal annealing temperatures, the films crystallize and dewet exposing the water monolayer but not the metal substrate. Figure 6 shows the isothermal desorption of an initially amorphous 75 ML D_2O film on Pt(111) (solid line). At 155 K, the film rapidly crystallizes as indicated by the decrease in the desorption rate.[26,33] After the crystallization is complete (t>75 s), the desorption rate remains constant until t~800 s, indicating zero order desorption from the crystalline ice film. The water coverage as a function of time can be calculated from the isothermal desorption spectrum (dashed line). Since the desorption rate is nearly constant after the film has crystallized, the coverage decreases approximately linearly with time. In a separate set of experiments, the isothermal desorption was stopped after various annealing intervals and the water film was examined with Kr TPD to determine the fraction of the surface covered by only 1 ML of water, F1 (Fig. 6, triangles). Immediately after the film has crystallized, the entire surface remains covered with at least 2 ML of water. However, further annealing results in additional water desorption and concomitant dewetting of the film: After ~350 s, when ~45 ML of water remain, the water monolayer becomes exposed and its fractional area, F1, increases with time until ~950 s when all of the multilayer ice crystallites have desorbed. The more tightly bound water monolayer subsequently desorbs, and the fraction of Pt(111) not covered by any water, F0, increases (Fig. 6, circles). Zero order isothermal desorption is also observed for initially nonwetting CI films (data not shown).

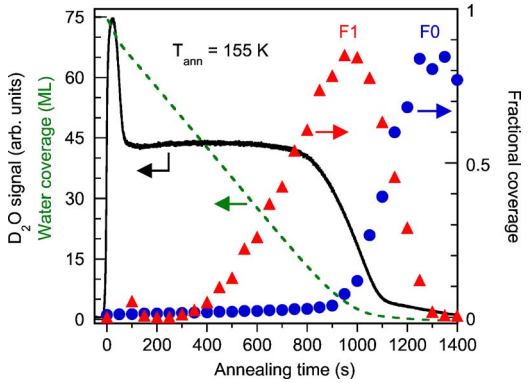

FIG. 6. (Color online) D_2O desorption rate (solid line), D_2O coverage (dashed line), F0 (circles) and F1 (triangles) versus annealing time for a 75 ML film deposited at 80 K and annealed at 155 K. After crystallizing, the D_2O desorption rate is constant indicating zero order desorption kinetics. However, the fraction of the surface covered with only 1 ML of water, F1, increases as the film dewets.

Zero order desorption kinetics has long been considered a good indicator that water films wet the substrate.[1,2,26,33] However, the present results show that zero order desorption kinetics can be obtained from nonwetting CI films. For example, in Fig. 6, the isothermal desorption rate is constant while the fraction of the surface covered with only 1 ML of water, F_1, increases. Analogous to the case for submonolayer adsorbate coverages on many surfaces,[14,36] zero order desorption kinetics is obtained for the nonwetting CI films as long as quasiequilibrium is maintained between the ice crystallites and the water monolayer via a mobile two dimen-

sional (2D) gaslike phase having the same chemical potential as the three dimensional (3D) ice crystallites.

Achieving quasiequilibrium between ice crystallites and a 2D gas phase probably depends, in part, upon the strength of the interaction of the monomers with the substrate and the distance between ice crystallites. If the interaction is too weak, the typical diffusion length for an admolecule prior to desorption can be less than the typical spacing between ice crystallites. In that case, quasiequilibrium will not be maintained and nonzero order desorption would be expected. For example, based on water TPD from Au(111), the first layer of water does not wet the surface, indicating that the interaction of the monomer with the surface is relatively weak. In that case, nonzero order desorption is observed for crystalline ice films desorbing from Au(111).[33]

C. Collision induced sputtering of CI films and monolayer refilling

The data in Figs. 5 and 6 show that the minimum energy configuration for multilayer CI films is nonwetting ice crystallites coexisting with an exposed hydrophobic water monolayer that wets the Pt(111) surface. As a further test, we prepared samples such that there were isolated ice crystallites surrounded by bare Pt(111) at low temperatures. If the surface having the exposed water monolayer and 3D ice crystallites is the equilibrium configuration, then the water molecules should diffuse off the ice crystallites to refill the water monolayer regions upon heating. To prepare surfaces with ice crystallites on bare Pt(111), we made use of previous research that has shown that thin water films can be sputtered by energetic atoms produced in a seeded molecular beam.[37] That work demonstrated that the sputtering yield for coverages less than ~3 ML is significantly higher than for thicker films. Since, as described above, the ice crystallites have an average thickness greater than 3 ML, the regions of the sample with the exposed water monolayer are preferentially sputtered compared to the ice crystallites, exposing bare Pt(111) while leaving the ice crystallites. The sample can then be subsequently heated and the refilling of the bare Pt(111) regions monitored using Kr TPD.

For the monolayer refilling experiments, D_2O CI films were grown at 150 K. Energetic Xe atoms were used to sputter the water monolayer away from those portions of the surface not covered by the ice crystallites. To produce the energetic Xe atoms, a molecular beam of ~0.5% Xe seed in He was expanded through a 100 μm diameter aperture at ~900 Torr and a temperature of ~870 K. These expansion conditions produce a supersonic Xe beam with an average kinetic energy of ~5.3 eV. Using ASW films that grow approximately layer by layer for at least the first 3 ML,[16] we verified that the Xe atoms efficiently sputter 1 ML thick films but not thicker films (data not shown).

Figure 7(a) shows the Kr TPD spectra from bare Pt(111) (dotted line), ~4 ML crystalline ice deposited at 150 K before sputtering (dashed line), and that same crystalline ice after sputtering with the Xe beam (solid line). For this experiment, ice crystallites initially cover ~55% of the surface. The absence of the high temperature, W0, peak in the Kr TPD spectra from the as grown ice sample demonstrates that

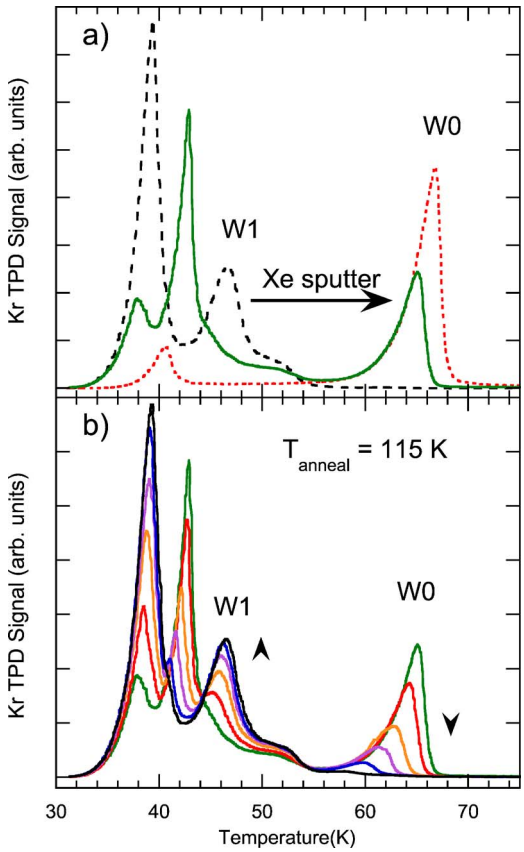

FIG. 7. (Color online) (a) Kr TPD spectra from bare Pt(111) (dotted line), 4 ML CI on Pt(111) (dashed line), and the same 4 ML CI film after sputtering with ~5.3 eV Xe atoms (solid line). Sputtering with Xe removes the water monolayer and exposes portions of the Pt(111) substrate as seen by the disappearance of the W1 peak and the appearance of the W0 peak. (b) Kr TPD spectra from a Xe sputtered, 4 ML CI film after zero, one, three, five, seven, and nine annealing cycles to 115 K. As the number of annealing cycles increases, the W0 peak decreases and the W1 peak increases, indicating that the bare Pt(111) regions are refilled by the water monolayer.

the Pt(111) is completely covered. After exposing this surface to the Xe beam at 80 K, the W1 peak corresponding to Kr desorbing from one layer of water is eliminated, being replaced by prominent peaks due to one and two layers of Kr desorbing from bare Pt(111) at ~65 K and ~43 K, respectively.[38] After Xe sputtering but prior to obtaining the first Kr TPD spectrum, the sample is heated to 100 K for 30 s to desorb any Xe which adsorbed during the sputtering. Separate experiments indicate that the extent of water diffusion at 100 K is negligible (data not shown). Comparison of the W0 peak area from the Xe sputtered ice surface to that from the clean Pt(111) shows that in the former case, ~45% of the surface is bare Pt(111) with the rest covered by ice crystallites. Thus the results show that energetic Xe atoms efficiently sputter the water monolayer as expected. They also show that for temperatures below 100 K, water molecules do not diffuse fast enough to refill the bare Pt regions on the time scale of this experiment (~100 s).

Water molecules do begin to diffuse off the ice crystallites and onto the Pt at higher temperatures. Figure 7(b) shows a series of Kr TPD spectra from a Xe sputtered sample as it is repeatedly annealed to 115 K. A surface with ice crystallites and bare Pt(111) was prepared, and the first

Kr TPD spectrum was obtained as described above. The temperature ramp rate was 0.5 K/s for the Kr TPD, and the temperature ramp was continued to 115 K. At that point the heater was turned off and the next Kr TPD spectrum (also with a ramp of 0.5 K/s to 115 K) was obtained after the sample cooled to ~28 K. Concomitant with the disappearance of the Kr TPD peaks at ~65 and 43 K associated with bare Pt, the peaks due to Kr desorbing from the water monolayer (~48 K) and CI (~38 K) reemerge [Fig. 7(b)]. In particular, as the number of annealing cycles increases, the W0 peak monotonically decreases and the W1 peak increases until a Kr TPD spectrum that is nearly identical to the spectrum from the unsputtered surface is obtained. Similar results have been obtained for a variety of initial water coverages and for several different annealing temperatures (data not shown). These results demonstrate that even at temperatures well below the temperatures required to *grow* crystalline ice, it is energetically favorable for the water molecules to diffuse off the ice crystallites and refill the bare Pt(111) regions with a single adsorbed water layer.

The Xe sputtering experiments further confirm that nonwetting 3D ice crystallites grow at the same time that other portions of the Pt(111) substrate remain covered by one and only one layer of water. These experiments show that even for water films where the total coverage is relatively high (e.g., 15–20 ML), the bare Pt(111) surface is easy to expose via Xe sputtering. Notably, while the fraction of the surface covered by only one layer of water decreases as the water coverage increases, the time required to expose those portions of the underlying Pt(111) substrate surface is *independent* of the water coverage. Furthermore, the amount of Kr desorbing from bare Pt after sputtering closely tracks the amount of Kr desorbing from the water monolayer before sputtering. Since the Xe does not efficiently sputter areas of the surface that are covered with more than 1 ML of water, these results show that ice films do not uniformly cover the surface in our experiments. Instead, the nonwetting ice crystallites cover more of the surface as the total coverage increases, but what is left is covered with only a single layer of water.

D. Ice crystallite distribution

While the results in Fig. 3 show that crystalline ice films do not wet the water monolayer on either Pt(111) or Pd(111), the size and distribution of the ice crystallites on the water monolayer are not obvious from the data. However, by making one primary assumption about the growth of the ice crystallites on these surfaces, we can use a simple model to estimate the average number of crystallites per unit area and thus the typical spacing between crystallites. In particular, we assume that the ice crystallites grow with a self-similar shape such that the ratios of the dimensions of the crystallites are independent of the amount of material in the crystallite. This assumption is plausible for the initial stages of growth where the ice crystallites are not yet impinging on each other.

Self-similar ice crystallite growth leads to a particular scaling relationship for F_1 versus the water coverage of the ice crystallites, θ_{CI}, which is independent of the actual shape

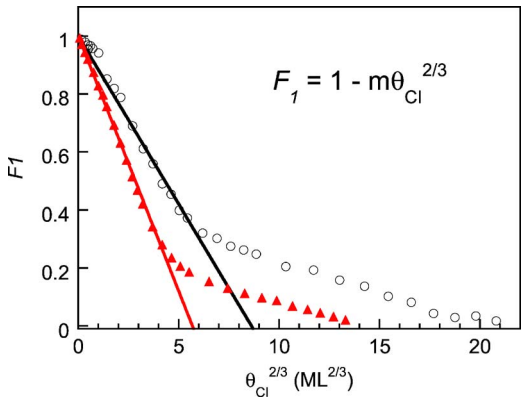

FIG. 8. (Color online) F_1 versus $\theta_{CI}^{2/3}$ for D_2O on Pt(111) (triangles) and H_2O on Pd(111) (circles). The lines are linear fits to the data (for $F_1 > 0.25$ or $F_1 > 0.35$ for Pt or Pd, respectively). As discussed in the text, the slopes of the lines are related to the average number of ice crystallites per unit area in the films.

of the ice crystallites. The basic point is that the volume of the ice crystallites is proportional to W^3, while the area in contact with the water monolayer is only proportional to W^2, where W is a characteristic linear dimension (i.e., size) of the crystallites. Therefore, as the average crystallite size increases, F_1 should decrease as $\theta_{CI}^{2/3}$. Figure 8 shows data from Fig. 3 replotted as F_1 vs $\theta_{CI}^{2/3}$ for H_2O on Pd(111) and D_2O on Pt(111). For both substrates, the data are approximately linear for F_1 greater than ~0.3–0.4. Thus the experimental results support the assumption of self-similar growth for the ice crystallites, at least initially (e.g., for $\theta < \sim 10$ ML).

From the initial slopes of F_1 vs $\theta_{CI}^{2/3}$, we can extract estimates for the average number of crystallites per unit area, σ, in the films. For simplicity we assume that the ice crystallites are all hemispheres of the same size.[39] The amount of water contained in the ice crystallites per unit area on the surface, V, is then

$$V = 2\pi\sigma R^3/3, \tag{1}$$

where R is the hemisphere radius. The volume of water per unit area is also related to the amount of water deposited on the surface: $V = h\theta_{CI}$, where h is the height per monolayer in the ice crystallites and θ_{CI} is the coverage for the ice crystallites. Since the first monolayer wets the surface, $\theta_{CI} = \theta - 1$. Combining these two results gives the crystallite radius as a function of θ_{CI},

$$R = \left(\frac{3\theta_{CI}h}{2\pi\sigma}\right)^{1/3}. \tag{2}$$

The fraction of the surface covered by the ice crystallites, F_{CI}, is $F_{CI} = \pi\sigma R^2$, and

$$F_1 = 1 - F_{CI} = 1 - \pi\sigma R^2. \tag{3}$$

Substituting the equation for $R(\theta_{CI})$ [Eq. (2)] into the equation for F_1 [Eq. (3)] gives the desired relationship between F_1 and θ_{CI},

$$F_1 = 1 - \left(\frac{9\pi h^2 \sigma}{4}\right)^{1/3} \theta_{CI}^{2/3} = 1 - m\theta_{CI}^{2/3}. \quad (4)$$

Thus, for self-similar crystallites, F_1 vs $\theta_{CI}^{2/3}$ should be a straight line, and the slope of the line, m, is related to the average number of crystallites per unit area: $\sigma = 4m^3/9\pi h^2$. If a different shape is assumed for the ice crystallites, σ will still be proportional to m^3, but the proportionality constant will be different. For example, for a hexagonal column (with a flat top) of diameter $2x$ and height βx, the corresponding result is $\sigma = 2\beta^2 m^3/3\sqrt{3}h^2$.

Using the spacing between crystalline bilayer planes along the c axis in crystalline ice for h ($h=0.365$ nm) and the measured values of m [$m=0.17$ and 0.12 for Pt(111) and Pd(111), respectively], we find $\sigma \sim 2\times 10^{-3}$ nm^{-2} for Pd(111) and $\sigma \sim 5\times 10^{-3}$ nm^{-2} for Pt(111). The typical lateral distance between the centers of the crystallites, l, should scale as $l \sim \sigma^{-1/2}$. Therefore this model suggests that $l \sim 22$ nm for Pd(111) and $l \sim 14$ nm for Pt(111). Since the specific values for σ and l extracted from the data depend on the shape that is assumed for the ice crystallites, and this simple model ignores many potential complications, the values for the typical spacing between ice crystallites should be considered as rough estimates. For example, for the case of hexagonal columns with $\beta=1$, the corresponding values would be $l \sim 14$ nm for Pd(111) and $l \sim 8.4$ nm for Pt(111). The key point is that the data and the model suggest that the typical spacing between crystallites is large compared to the size of the unit cell for the water monolayer on either surface.

The model described above should only be valid for the initial stages of growth where the ice crystallites do not impinge upon each other. However, in Fig. 8, the data are approximately linear over a surprisingly large range: $F_1 > \sim 0.27$ for Pt(111) and $> \sim 0.33$ for Pd(111). For a random distribution of crystallites, Monte Carlo simulations of ice nucleation and growth (not shown) indicate that a plot of F_1 vs $\theta^{2/3}$ should display noticeable departures from linearity for $F_1 < \sim 0.65$. Hence, the experimental results suggest some degree of lateral ordering for the ice crystallites. For perfectly ordered arrays of monodispersed hemispheres, F_1 vs $\theta^{2/3}$ would be linear until the hemispheres begin to impinge upon each other. It is straightforward to show that this occurs when $F_1=0.215$ for a square or 0.094 for a hexagonal array. Additionally, the experimental data in Fig. 8 exhibit approximately linear behavior for higher coverages as well, albeit with a reduced slope. We have unsuccessfully explored several simple models in an attempt to explain this observation. Nonetheless, the data indicate that the substrate is not completely covered until the average film thickness is large. Clearly, real space images of these films would be invaluable for understanding the experimental findings.

E. Comparison to other studies

The nonwetting growth of crystalline ice on the water monolayer on both Pt(111) and Pd(111) suggests that the surface free energies of the water monolayer on both substrates are smaller than the surface free energy of crystalline ice. Thus the structures of the water monolayer and the crystalline ice surfaces, which determine the surface free energies, are important factors influencing the film morphology.

The structure of the water monolayer grown at relatively high temperatures (e.g., $T > 100$ K) on Pt(111) has been investigated by low energy electron diffraction (LEED),[13,27,40,41] scanning tunneling microscopy (STM),[19] helium atom scattering (HAS),[12] and sum frequency generation (SFG).[42] While several different structures have been reported, the most recent HAS and LEED experiments have found an ordered overlayer with a $(\sqrt{39}\times\sqrt{39})R16°$ unit cell.[12,13,27] However, the detailed arrangement of water molecules within this unit cell is not known.[43]

Structures with a low surface free energy are not expected to have a large number of broken (or dangling) bonds. In many cases, surfaces reconstruct to minimize the number of dangling bonds.[44] For the water monolayer on metals such as Pt(111) and Pd(111), essentially all the water molecules are hydrogen bonded to three neighbors in a plane approximately parallel to the surface. About half the molecules are also bound to the substrate through one of the oxygen lone electron pairs and are thus fully coordinated.[12,43] For the other molecules—those not bound to the substrate through the oxygen lone pair—early models proposed that they formed dangling OH groups pointing away from the surface,[2] and SFG results appear to be consistent with this picture.[42] However, several recent experimental results are consistent regarding the dangling OH bonds: X-ray absorption[17] and Fourier transform infrared[27] (FTIR) studies of the water monolayer on Pt(111) indicate that most of the molecules not bound to the surface through the oxygen adopt a H-down configuration where a H atom "bonds" to the surface. Thus experiments indicate that there is a significant energy cost associated with dangling bonds of a H-up configuration for the water monolayer on Pt(111). Density-functional theory (DFT) calculations[17,18,43,45,46] also suggest that the molecules not bound to the surface through their oxygen adopt a H-down configuration.

Compared to Pt(111), considerably less is known about the adsorption of water on Pd(111).[1] DFT calculations suggest that the basic substrate-adsorbate interactions are quite comparable on Pt(111) and Pd(111).[18,45] While we are unaware of any experimental reports of the structure of a complete monolayer on Pd(111), the structure of submonolayer water films has been investigated with scanning tunneling microscopy and DFT calculations.[15] In that case, the water molecules form islands that are built up primarily from planar water hexamers where the oxygen atoms are all at the same height above the surface and the hydrogen bonds are in a plane parallel to the surface.[15] The water molecules which connect the flat-lying hexamers to make larger islands are also apparently H down. So it appears that all (or almost all) the water molecules interact significantly with the substrate on both Pt(111) and Pd(111), and the water monolayer has few dangling OH groups or oxygen lone pair electrons protruding into the vacuum.

For crystalline ice films at the temperatures relevant for UHV studies (i.e., $T < \sim 155$ K), the structure of the surface is controversial. HAS (Ref. 47) and LEED (Ref. 48) indicate that the oxygen atoms occupy the lattice sites expected for

perfect termination of bulk crystalline ice [corresponding to the (0001) face of I_h or the (111) face of I_c] but perhaps with enhanced vibrational amplitudes for the outer layer of water molecules. The important point is that a bulk terminated surface of crystalline ice will have a high density of broken bonds resulting in a high surface free energy. In fact, SFG spectra of thin crystalline ice films on Pt(111) have a dangling OH feature that apparently does not change appreciably with the film thickness.[42] However, in contrast to the HAS, LEED, and SFG experiments, FTIR and coadsorption studies[49,50] found few dangling OH bonds for crystalline ice films, suggesting a reconstructed surface. Whatever the structure of the ice surface is, the observed nonwetting growth of crystalline ice on Pt(111) and Pd(111) indicates that the water monolayer structure on both surfaces has a lower surface free energy than crystalline ice.

Recently Hodgson and co-workers have used LEED, FTIR, water thermal desorption and chloroform adsorption/desorption to investigate the structure of thin crystalline ice films on Pt(111).[27,51] Based on their observations, they propose that ice crystallites nucleate in an ordered array with preferred nucleation sites within the $\sqrt{39}$ monolayer on Pt(111).[27,51] As film thickness increases, the films grow commensurate with the $\sqrt{39}$ structure of the water monolayer. Aggregation of the crystallites leads to increasing disorder in the films such that the $(\sqrt{39}\times\sqrt{39})R16°$ LEED pattern slowly fades. For films thicker than ~40 ML, bulk ice is more stable and the films convert to this structure.

Comparison of our results with those of Hodgson and co-workers shows many similarities. However, there are some discrepancies in the interpretations of the results. As already mentioned, they suggest that ice nucleates in an ordered array associated with sites in every $\sqrt{39}$ unit cell on the surface. Support for this contention is found in STM studies of water on Pt(111), where it was suggested that the second layer of water nucleates at specific sites within each unit cell on the water monolayer.[19] However, the STM results were obtained at lower growth temperatures than those studied here and may not reflect the true equilibrium configuration for coverages greater than 1 ML. The fraction of the surface covered with only one layer of water, F_1, versus the total water coverage also suggests that closely spaced crystallites are unlikely for our samples: From F_1 versus coverage (Fig. 3), we can extract what the typical dimensions for the ice crystallites would have to be if they nucleated in every unit cell. For example, F_1 is ~0.15 at θ=2 ML on Pt(111). Therefore, since the $(\sqrt{39}\times\sqrt{39})R16°$ unit cell should contain ~32 water molecules,[12,43] only ~5 (i.e., $\sim 0.15\times 32$) of the molecules in the unit cell would be covered by the ice crystallites if they nucleated in each unit cell. However, the average height of these crystallite "towers" would be ~7 layers high ($=1/F_1$). By the same reasoning, a hexagonal column with a base of six molecules would need to be ~6 layers high. It seems unlikely that such thin, high surface area crystallites would be stable. As discussed above, a simple model of the film growth predicts that the average distance between ice crystallites in our CI films is ~8–14 nm for Pt(111) (see Fig. 8)—much larger than the size of the $\sqrt{39}$ unit cell. Here again, a real space probe will be invaluable for determining the actual film morphology.

IV. CONCLUSION

In summary, we have used rare gas physisorption to investigate water growth on Pt(111) and Pd(111). The first water layer wets both Pt(111) and Pd(111), as expected. Surprisingly, the water monolayer on each substrate is *hydrophobic* and gives rise to *nonwetting growth* for subsequent crystalline layers. A simple model suggests that initially the ice crystallites are well separated with typical spacings of ~14 nm or more. Thin wetting ASW films dewet when they are heated to higher temperatures to induce crystallization. The temperature at which films dewet increases with increasing film thickness and is correlated with the temperature at which the films crystallize. For crystalline ice films that have been sputtered with Xe atoms to expose portions of the Pt(111) substrate, water monomers readily diffuse off the ice crystallites to reform the water monolayer at temperatures as low as 115 K. The results indicate that Pt(111) and Pd(111) are not good templates for growing smooth, extended epitaxial crystalline ice films in a layer-by-layer fashion. Furthermore, the observation of zero order water desorption kinetics cannot be used to infer that multilayer water films wet the substrate.

ACKNOWLEDGMENTS

This work was supported by the U.S. Department of Energy, Office of Basic Energy Sciences, Chemical Sciences Division. Experiments were performed in the W.R. Wiley Environmental Molecular Sciences Laboratory at the Pacific Northwest National Laboratory which is operated for the U.S. Department of Energy by Battelle Memorial Institute under Contract No. DE-AC06-76RLO 1830.

[1] M. A. Henderson, Surf. Sci. Rep. **46**, 1 (2002).
[2] P. A. Thiel and T. E. Madey, Surf. Sci. Rep. **7**, 211 (1987).
[3] A. Verdaguer, G. M. Sacha, H. Bluhm, and M. Salmeron, Chem. Rev. (Washington, D.C.) **106**, 1478 (2006).
[4] A. W. Adamson, *Physical Chemistry of Surfaces*, 5th ed. (Wiley, New York, 1990).
[5] G. Gahl, U. Bovensiepen, C. Frischkorn, K. Morgenstern, K.-H. Rieder, and M. Wolf, Surf. Sci. **532–535**, 108 (2003).
[6] J. M. K. Donev, Q. Yu, B. R. Long, R. K. Bollinger, and S. C. Fain, J. Chem. Phys. **123**, 044706 (2005).
[7] H. Bluhm and M. Salmeron, J. Chem. Phys. **111**, 6947 (1999).
[8] M. S. Westley, G. A. Baratta, and R. A. Baragiola, J. Chem. Phys. **108**, 3321 (1998).
[9] Z. Dohnálek, G. A. Kimmel, P. Ayotte, R. S. Smith, and B. D. Kay, J. Chem. Phys. **118**, 364 (2003).
[10] K. P. Stevenson, G. A. Kimmel, Z. Dohnálek, R. S. Smith, and B. D. Kay, Science **283**, 1505 (1999).
[11] G. A. Kimmel, K. P. Stevenson, Z. Dohnálek, R. S. Smith, and B. D. Kay, J. Chem. Phys. **114**, 5284 (2001).
[12] A. Glebov, A. P. Graham, A. Menzel, and J. P. Toennies, J. Chem. Phys. **106**, 9382 (1997).
[13] S. Haq, J. Harnett, and A. Hodgson, Surf. Sci. **505**, 171 (2002).
[14] J. L. Daschbach, B. M. Peden, R. S. Smith, and B. D. Kay, J. Chem. Phys. **120**, 1516 (2004).
[15] J. Cerda, A. Michaelides, M. L. Bocquet, P. J. Feibelman, T. Mitsui, M. Rose, E. Fomin, and M. Salmeron, Phys. Rev. Lett. **93**, 116101 (2004).
[16] G. A. Kimmel, N. G. Petrik, Z. Dohnálek, and B. D. Kay, J. Chem. Phys. **125**, 044713 (2006).

[17] H. Ogasawara, B. Brena, D. Nordlund, M. Nyberg, A. Pelmenschikov, L. G. M. Pettersson, and A. Nilsson, Phys. Rev. Lett. **89**, 276102 (2002).
[18] A. Michaelides, A. Alavi, and D. A. King, Phys. Rev. B **69**, 113404 (2004).
[19] M. Morgenstern, J. Muller, T. Michely, and G. Comsa, Z. Phys. Chem. **198**, 43 (1997).
[20] Z. Dohnálek, J. Kim, and B. D. Kay, Surf. Sci. **600**, 3461 (2006).
[21] M. Han, P. Mrozek, and A. Wieckowski, Phys. Rev. B **48**, 8329 (1993).
[22] G. A. Kimmel, N. G. Petrik, Z. Dohnálek, and B. D. Kay, Phys. Rev. Lett. **95**, 166102 (2005).
[23] H. Schlichting and D. Menzel, Surf. Sci. **272**, 27 (1992).
[24] G. A. Kimmel, M. Persson, Z. Dohnálek, and B. D. Kay, J. Chem. Phys. **119**, 6776 (2003).
[25] L. W. Bruch, M. W. Cole, and E. Zaremba, *Physical Adsorption: Forces and Phenomena* (Clarendon, Oxford, 1997).
[26] P. Löfgren, P. Ahlström, D. V. Chakarov, J. Lausmaa, and B. Kasemo, Surf. Sci. Lett. **367**, L19 (1996).
[27] G. Zimbitas, S. Haq, and A. Hodgson, J. Chem. Phys. **123**, 174701 (2005).
[28] M. Wolf, S. Nettesheim, J. M. White, E. Hasselbrink, and G. Ertl, J. Chem. Phys. **92**, 1509 (1990).
[29] M. Wolf, S. Nettesheim, J. M. White, E. Hasselbrink, and G. Ertl, J. Chem. Phys. **94**, 4609 (1991).
[30] For the results presented here, the important point is that the ASW films cover the water monolayer. As discussed in Ref. 16, the underlying reasons for this behavior, while not fully understood, may have both kinetic and energetic origins.
[31] Z. Dohnálek, R. L. Ciolli, G. A. Kimmel, K. P. Stevenson, R. S. Smith, and B. D. Kay, J. Chem. Phys. **110**, 5489 (1999).
[32] Z. Dohnálek, G. A. Kimmel, R. L. Ciolli, K. P. Stevenson, R. S. Smith, and B. D. Kay, J. Chem. Phys. **112**, 5932 (2000).
[33] R. S. Smith, C. Huang, E. K. L. Wong, and B. D. Kay, Surf. Sci. Lett. **367**, L13 (1996).
[34] R. J. Speedy, P. G. Debenedetti, R. S. Smith, C. Huang, and B. D. Kay, J. Chem. Phys. **105**, 240 (1996).
[35] R. S. Smith, C. Huang, E. K. L. Wong, and B. D. Kay, Phys. Rev. Lett. **79**, 909 (1997).
[36] K. J. Wu, L. D. Peterson, G. S. Elliott, and S. D. Kevan, J. Chem. Phys. **91**, 7964 (1989).
[37] Y. Lilach, L. Romm, T. Livneh, and M. Asscher, J. Phys. Chem. B **105**, 2736 (2001).
[38] Since the second layer of Kr on Pt(111) is more stable than the first layer of Kr on the ice crystallites, the nominal ~1.2 ML Kr adsorbs in two layers on the bare Pt(111) regions of the sample with the remainder adsorbing on the ice crystallites and producing the small peak at ~38 K in the Kr TPD.
[39] Note that the shape assumed for the ice crystallites does not qualitatively change the model, while it does influence the specific numbers extracted from the model for the average spacing of ice crystallites.
[40] L. E. Firment and G. A. Somorjai, J. Chem. Phys. **63**, 1037 (1975).
[41] G. B. Fisher and J. L. Gland, Surf. Sci. **94**, 446 (1980).
[42] X. C. Su, L. Lianos, Y. R. Shen, and G. A. Somorjai, Phys. Rev. Lett. **80**, 1533 (1998).
[43] P. J. Feibelman, Phys. Rev. Lett. **91**, 059601 (2003).
[44] A. Zangwill, *Physics At Surfaces* (Cambridge University Press, Cambridge, 1988).
[45] S. Meng, E. G. Wang, and S. W. Gao, Phys. Rev. B **69**, 195404 (2004).
[46] T. Jacob and W. A. Goddard, J. Am. Chem. Soc. **126**, 9360 (2004).
[47] A. Glebov, A. P. Graham, A. Menzel, J. P. Toennies, and P. Senet, J. Chem. Phys. **112**, 11011 (2000).
[48] N. Materer, U. Starke, A. Barbieri, M. A. VanHove, G. A. Somorjai, G. J. Kroes, and C. Minot, Surf. Sci. **381**, 190 (1997).
[49] J. E. Schaff and J. T. Roberts, J. Phys. Chem. **100**, 14151 (1996).
[50] J. E. Schaff and J. T. Roberts, J. Phys. Chem. **98**, 6900 (1994).
[51] G. Zimbitas and A. Hodgson, Chem. Phys. Lett. **417**, 1 (2006).